

## Universal Bound to the Amplitude of the Vortex Nernst Signal in Superconductors

Carl Willem Rischau<sup>1,\*</sup>, Yuke Li<sup>1,†</sup>, Benoît Fauqué<sup>2</sup>, Hisashi Inoue<sup>3,‡</sup>, Minu Kim<sup>3,§</sup>,  
 Christopher Bell<sup>3,||</sup>, Harold Y. Hwang<sup>3</sup>, Aharon Kapitulnik<sup>3</sup>, and Kamran Behnia<sup>1,¶</sup>  
<sup>1</sup>*Laboratoire de Physique et d'Étude des Matériaux (ESPCI Paris—CNRS—Sorbonne Université),  
 PSL Research University, 75005 Paris, France*  
<sup>2</sup>*JEIP, USR 3573 CNRS, Collège de France, PSL Research University, 75005 Paris, France*  
<sup>3</sup>*Geballe Laboratory for Advanced Materials, Stanford University, Stanford, California 94305, USA*

 (Received 13 August 2020; revised 5 November 2020; accepted 7 January 2021; published 16 February 2021)

A liquid of superconducting vortices generates a transverse thermoelectric response. This Nernst signal has a tail deep in the normal state due to superconducting fluctuations. Here, we present a study of the Nernst effect in two-dimensional heterostructures of Nb-doped strontium titanate (STO) and in amorphous MoGe. The Nernst signal generated by ephemeral Cooper pairs above the critical temperature has the magnitude expected by theory in STO. On the other hand, the peak amplitude of the vortex Nernst signal below  $T_c$  is comparable in both and in numerous other superconductors despite the large distribution of the critical temperature and the critical magnetic fields. In four superconductors belonging to different families, the maximum Nernst signal corresponds to an entropy per vortex per layer of  $\approx k_B \ln 2$ .

DOI: [10.1103/PhysRevLett.126.077001](https://doi.org/10.1103/PhysRevLett.126.077001)

Superconducting vortices are quanta of magnetic flux with a normal core surrounded by a whirling flow of Cooper pairs [1]. In a “vortex liquid” a charge current and an electric field can be simultaneously present and produce dissipation. This state of matter is prominent in high- $T_c$  cuprates [2]. One property of the vortex liquid is a finite Nernst effect (the generation of a transverse electric field by a longitudinal thermal gradient) [3]. Together with its Ettingshausen counterpart (a transverse thermal gradient produced by a longitudinal charge current), it has been widely documented in both conventional [4] and high- $T_c$  superconductors [5–7]. In the latter case, the debate has been mostly focused on interpreting the persistence of a Nernst signal above the critical temperature [7–9]. The vortex origin of the peak signal below  $T_c$  remains undisputed and its quantitative amplitude unexplained. Theoretical tradition has linked the magnitude of the finite Nernst signal to the motion of vortices under the influence of a thermal gradient due to the excess entropy of the normal core [4,10–12]. As a consequence, the magnitude of the Nernst response is expected to strongly vary among different superconductors [10–12].

Here we present a study of the Nernst effect in two superconductors, namely, two-dimensional Nb-doped SrTiO<sub>3</sub> and  $\alpha$ -MoGe. We will show that the magnitude of the fluctuating Nernst response above  $T_c$  is in agreement with theoretical expectations, but not the amplitude of the vortex Nernst signal in the flux flow regime below the critical temperature. Putting under scrutiny available data for other superconductors (with a range of critical temperatures extending over 3 orders of magnitude), we find that the observed peak does not exceed a few  $\mu\text{V}/\text{K}$ . Available

theories [10–12] link the amplitude of the vortex Nernst response in a given superconductor to its material-dependent length scales in disagreement with our observation.

Figure 1 presents our data on two-dimensional Nb-doped strontium titanate (STO). The heterostructure consisted of 1% at. Nb: SrTiO<sub>3</sub> ( $n_{2D} = 8.6 \times 10^{13} \text{ cm}^{-2}$ ) with a thickness of 4.5 nm sandwiched by cap and buffer undoped STO layers [see Fig. 1(a)]. Previous studies documented the normal state [13,14] and the superconducting properties [15] of such  $\delta$ -doped samples in detail. Using a standard two-thermometers-one-heater setup [see Fig. 1(b)], we measured diagonal (resistivity and thermopower) as well as off-diagonal (Nernst and Hall effects) transport coefficients of the sample with the same electrodes (see the Supplemental Material [16] for more details). As seen in panels (d)–(j) of the same figure, a Nernst signal emerges in the vortex state and its peak shifts with magnetic field and remains close to the midpoint of the resistive transition.

Figure 2(a) shows the evolution of the low-field Nernst coefficient ( $\nu = N/B$ ) across  $T_c$ . Its magnitude is extremely sensitive to the magnetic field. The Nernst coefficient of the normal quasiparticles detected in bulk crystals of doped STO [17] is much smaller and has an opposite sign ( $\nu = -0.04 \mu\text{V}/\text{KT}$  at  $B = 1 \text{ T}$  and  $T = 0.5 \text{ K}$ ) [3,17]. It is negligible at  $B = 0.005 \text{ T}$ . As indicated by a recent study on NbSe<sub>2</sub> [18], confinement to two dimensions facilitates the observation of the superconducting contribution to the Nernst response.

Theoretically, the Nernst signal due to the Gaussian fluctuations of the superconducting order parameter [22–24] leads to a simple expression for the off-diagonal component of the thermoelectric tensor,  $\alpha_{xy}$ :

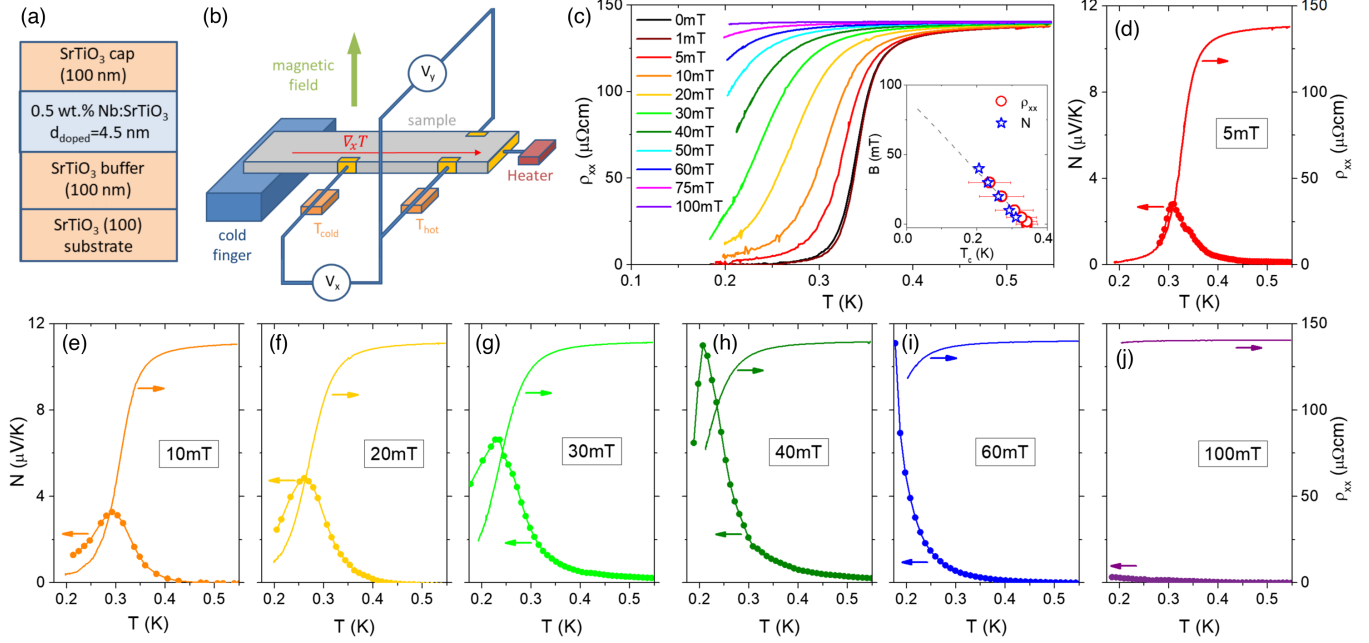


FIG. 1. The Nernst effect in two-dimensional Nb-doped strontium titanate: (a) Schematic view of the heterostructure. (b) Sketch of the two-thermometers–one-heater setup used in these measurements. (c) Resistivity  $\rho_{xx}$  as a function of temperature. The midpoint resistive transition at  $T_c = 0.341$  K shifts to lower temperatures with increasing magnetic field. The inset shows the correlated evolution of this midpoint and the Nernst peak with temperature and magnetic field. (d)–(j) The Nernst signal  $N$  and  $\rho_{xx}$  vs temperature at different magnetic fields, both the Nernst peak and the resistive transition vanish at  $B = 0.1$  T.

$$\frac{\alpha_{xy}^{Fl}}{B}(T) = \frac{k_B e^2}{6\pi\hbar^2} \xi^2(T). \quad (1)$$

Here,  $\xi(T) = \xi_0/\sqrt{\epsilon}$  is the superconducting coherence length and  $\epsilon = (T - T_c)/T_c$  is the reduced temperature. Combining our Nernst and resistivity data, we can plot  $\alpha_{xy}$  in Fig. 2(b). Its magnitude at twice  $T_c$  is compatible with what is expected by Eq. (1) and the zero-temperature coherence length extracted from the upper critical field ( $\xi_0 = 60$  nm) [13]. Similar observations were previously reported for amorphous superconductors [19,25,26] and in cuprates [20,21]. Because of the long  $\xi$ ,  $\alpha_{xy}$  found here is larger than those studied previously [see the inset in Fig. 2(b) and the Supplemental Material [16]].

We now turn our attention to the vortex Nernst signal below the critical temperature. The Nernst signal in Nb:STO peaks to  $\approx 11 \mu\text{V/K}$  [see Figs. 1(h), 1(i) and Fig. 4(b)]. At the temperature and magnetic field of this peak, the measured resistivity is  $\approx 100 \mu\Omega$  cm. Therefore, the peak transverse thermoelectric response is  $\alpha_{xy} = N/\rho = 11$  A/Km. In the traditional approach to the vortex dynamics [3,4,6], this is set by a balance between the thermal force (proportional to the entropy of each vortex,  $S_d$ ) and the Lorentz force proportional to its magnetic flux,  $\phi_0 = h/2e = 2.07 \times 10^{-15}$  Tm<sup>2</sup> [1]. This yields  $S_d = \phi_0 \times \alpha_{xy} \approx 2.3 \times 10^{-14}$  J/Km [16].

Sergeev and co-workers [12], after commenting the inadequacies of previous theories [10,11] (see the

Supplemental Material [16] for details) proposed the following expression for vortex transport entropy:

$$S_d^{\text{core}} \simeq -\pi\xi^2 \frac{\partial H_c^2}{\partial T} \frac{1}{8\pi}. \quad (2)$$

The right side of Eq. (2) is the product of the vortex size ( $\xi$  is the coherence length) and the entropy difference between the two competing phases. Indeed, the thermodynamic critical field  $H_c$  is set by the difference between the free energies of the normal  $F_n$  and the superconducting  $F_s$  phases set:  $H_c^2/8\pi = F_n - F_s$  [1]. Using the experimentally known coherence length and critical fields, Eq. (2) yields  $S_d = 1.2 \times 10^{-12}$  J/Km (see the Supplemental Material for details [16]), 50 times larger than the experimental value and indicating the absence of a crucial ingredient.

Figure 3 presents a study of the Nernst effect in another two-dimensional superconductor, namely, amorphous MoGe, a platform for studying superconductor-insulator transitions [27]. The Nernst peak evolves concomitantly with the resistive transition with increasing magnetic field. The vortex Nernst signal peak is slightly lower than the peak in Nb:STO. The extracted  $\alpha_{xy}$  ( $\approx 14$  A/Km) and  $S_d$  ( $\approx 2.8 \times 10^{-14}$  J/Km) are almost the same. In other words, these two superconductors, despite an almost 20-fold difference in their  $T_c$ 's (6.2 vs 0.34 K) and their  $H_{c2}$ s (7 vs 0.1 T) have similar entropy per vortex.

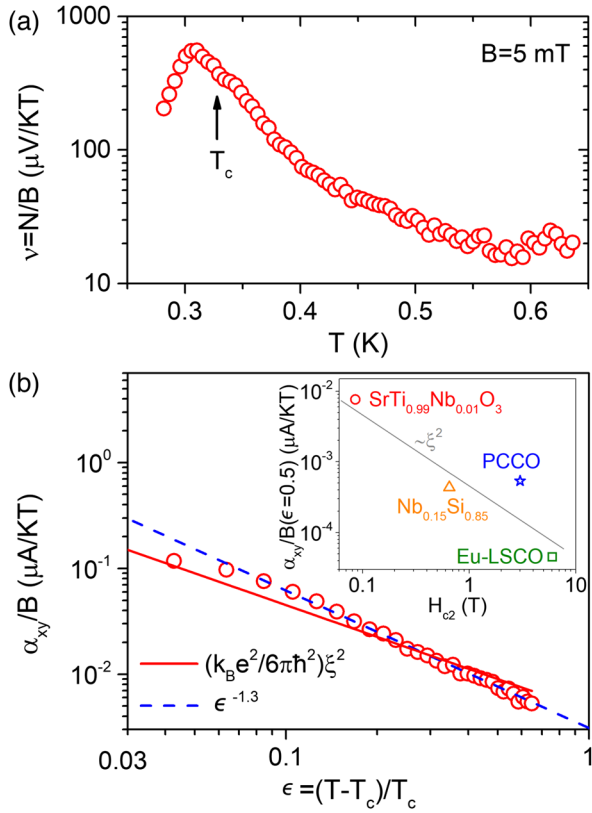


FIG. 2. The Nernst response in the normal state due to superconducting fluctuations: (a) The Nernst coefficient as a function of temperature in two-dimensional Nb:STO across the critical temperature at  $B = 5$  mT. (b) The off-diagonal component of the thermoelectric tensor,  $\alpha_{xy} = (N/\rho)a_0$  as a function of reduced temperature,  $\epsilon = (T - T_c)/T_c$ . The dashed line represents  $\epsilon^{-1.3}$ , the solid line what is expected by Eq. (1). The inset compares the magnitude of normal state  $\alpha_{xy}$  (at  $T = 1.5T_c$ ) in different superconductors [19–21] as a function of their upper critical field,  $H_{c2}$ . The dashed line represents the magnitude expected by Eq. (1) and a coherence length given by  $H_{c2}(0)$ .

Figure 4(a) shows the Nernst data in a number of superconductors. Some are layered, others isotropic. Some are crystalline, others amorphous. Some are conventional, others unconventional. Some were studied as thin films, others as single crystals. In spite of the large difference in the critical temperature, the Nernst signal in all peaks to a few  $\mu\text{V}/\text{K}$ . Figures 4(b)–4(d) compares the contours of  $N(T, B)$  in three different superconductors. The field and the temperature scales differ by 2 orders of magnitude, but the summit has a comparable magnitude of 4–10  $\mu\text{V}/\text{K}$ .

This similarity in the magnitude of the vortex Nernst response below  $T_c$  is to be contrasted with the material-dependent amplitude of the fluctuating Nernst signal above  $T_c$  and the material-dependent amplitude of the quasiparticle Nernst signal. The latter is known to spread over 6 orders of magnitude in different metals [3,8]. Theory gives a satisfactory account of the amplitude of the quasiparticle

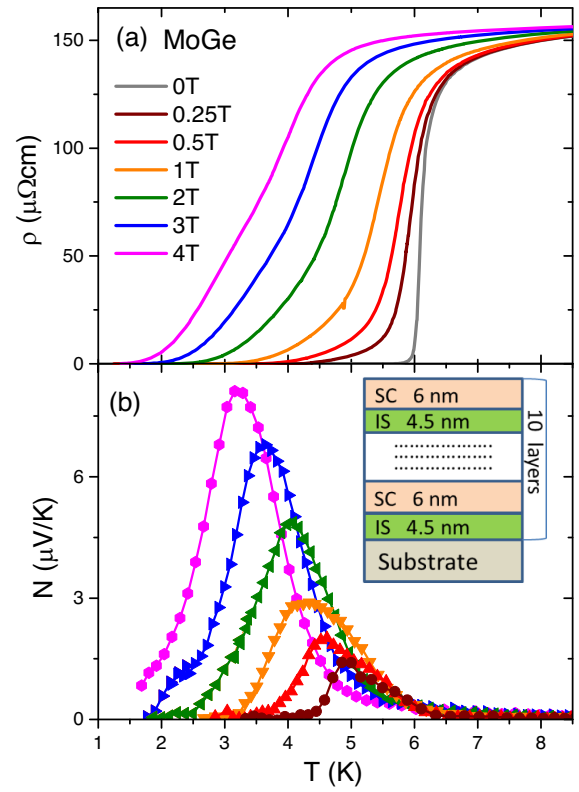


FIG. 3. Nernst effect in amorphous MoGe: (a) Evolution of the resistive superconducting transition in amorphous films of MoGe with magnetic field. (b) Nernst effect  $N$  in the same sample. The color code for magnetic fields is identical to the one used in the upper panel. The inset schematically depicts the structure of the sample consisting of alternating superconducting and insulating layers.

or the fluctuating Nernst signal but, as we saw above, not the vortex Nernst signal.

One defect of the common picture of the vortex Nernst signal is its neglect of forces other than the thermal force acting on a vortex as discussed in the Supplemental Material [16]. An upper boundary to  $N$  is equivalent to a lower boundary to the viscosity-to-entropy density ratio for the vortex liquid. Such a boundary is a subject of current interest [31,32] also discussed in the Supplemental Material [16].

Table I lists four different crystalline superconductors and their largest value of the Nernst signal at any field and temperature,  $N^{\text{peak}}$ . They belong each to a different family and they are chosen because the resistivity of the sample at  $N = N^{\text{peak}}$  (dubbed  $\rho^{\text{peak}}$ ) has been reported, allowing us to calculate the vortex entropy per layer, using the lattice parameter  $c$ :  $S_d^{\text{sheet}} = \Phi_0(N^{\text{peak}}/\rho^{\text{peak}})c$ . As seen in the table,  $S_d^{\text{sheet}}$  is similar and of the order of  $k_B \ln 2 = 0.95 \times 10^{-23}$  J/K. In other words, despite the dissimilarity in the coherence length and in the penetration depth, the entropy carried by each vortex per sheet is of the order of a Boltzmann constant.

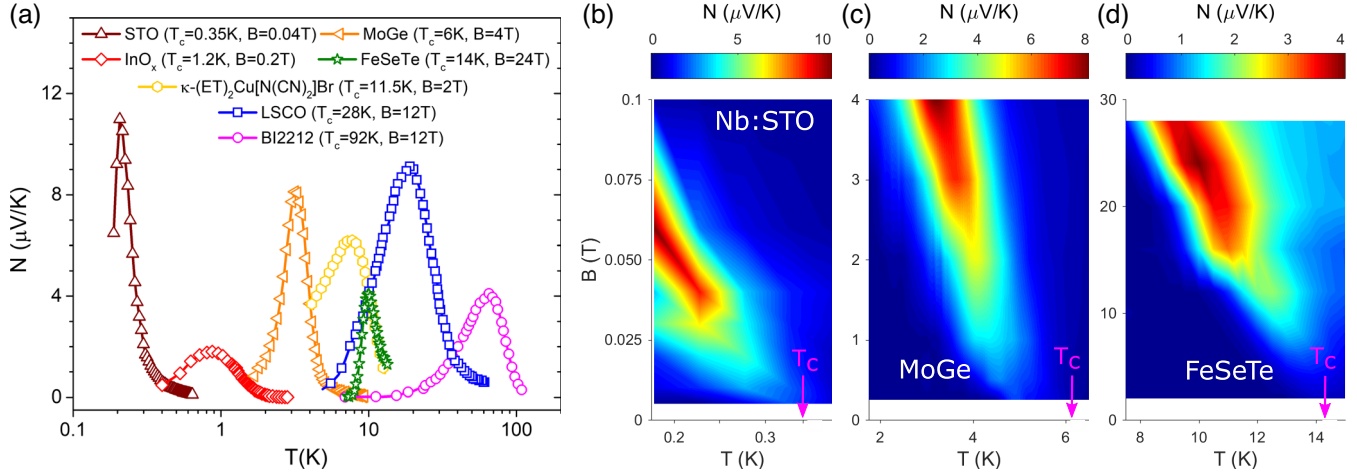


FIG. 4. Peak Nernst signal in different superconductors: (a) The Nernst signal as a function of temperature in STO and MoGe (present work) compared with data on an amorphous film of  $\text{InO}_x$  [26], on  $\text{FeSe}_{0.6}\text{Te}_{0.4}$  [28], on  $\kappa\text{-(ET)}_2\text{Cu[N(CN)}_2\text{]Br}$  [29], on  $\text{La}_{1.92}\text{Sr}_{0.08}\text{CuO}_4$  [30] and on  $\text{Bi}_2\text{Sr}_2\text{CaCu}_2\text{O}_{8+\delta}$  [6]. For each system, the critical temperature is indicated together with the magnetic field at which the observed peak was the largest. In all systems, this magnetic field is the one at which the peak is largest, except in Bi2212 [6], for which the data were restricted to 12 T. The field and temperature dependence of the Nernst signal are shown as color plots for (b) Nb:STO, (c) MoGe, and (d)  $\text{FeSe}_{0.6}\text{Te}_{0.4}$  [28]. Note the similarity in the peak amplitude in contrast to the large difference in the field and temperature scales.

Our observation implies that Eq. (2) does not give an accurate account of the mobile entropy of a superconducting vortex and the problem should be deeply reconsidered. At this stage, we can identify two obvious shortcomings with the equation. First it assumes that the entropy density in the vortex core is identical to the entropy density in the normal phase. This neglects the existence of the Caroli–de Gennes–Matricon [33] levels in the core. Second, it takes for granted that all core entropy is mobile and does not distinguish between what is bound to a mobile flux line and what is not.

To sum up, we find that in four superconductors with different normal states, pairing symmetries and critical temperatures, the Nernst transport entropy per vortex per

layer is of the order of  $k_B$ . We expect this to motivate experimental studies of the vortex Nernst signal in other superconductors of interest [34–36].

We thank H. Aubin, M. V. Feigel'man, S. A. Hartnoll, S. A. Kivelson, K. Trachenko, A. A. Varlamov, and G. E. Volovik for discussions. C. W. R. acknowledges the support of Fonds-ESPCI, Paris. This work was supported by a ‘QuantEmX’ Exchange Awards at Stanford University (K. B.) and at ESPCI (A. K.), by the Agence Nationale de la Recherche (ANR-18-CE92-0020-01; ANR-19-CE30-0014-04) and by Jeunes Equipes de l’Institut de Physique du Collège de France. H. I., M. K., C. B., and H. Y. H. were supported by the U.S. Department of Energy, Office of Basic Energy Sciences, Division of Materials Sciences and Engineering, under Contract No. DE-AC02-76SF00515. A. K. was supported by the National Science Foundation Grant No. NSF-DMR-1808385.

TABLE I. The peak Nernst signal in superconductors belonging to four different families:  $\text{SrTi}_{0.99}\text{Nb}_{0.01}\text{O}_3$  (Nb:STO),  $\text{FeSe}_{0.6}\text{Te}_{0.4}$  (FeSeTe) [28],  $\kappa\text{-(ET)}_2\text{Cu[N(CN)}_2\text{]Br}$  ( $\kappa\text{-ET}$ ) [29] and  $\text{La}_{1.92}\text{Sr}_{0.08}\text{CuO}_4$  (LSCO08) [30]. Also listed are sheet resistance per layer (resistivity divided by the lattice parameter along the orientation of magnetic field) measured at the temperature and the magnetic field corresponding to  $N = N^{\text{peak}}$  and the deduced entropy per vortex per layer (see the Supplemental Material [16] for a discussion of the available Nernst data).

Compound	$T_c$ [K]	$N^{\text{peak}}$ [ $\mu\text{V/K}$ ]	$c$ nm	$\rho^{\text{peak}}/c$ [k $\Omega$ ]	$S_{\text{sheet}}^{\text{vortex}}$ [ $10^{-23}$ J/K]
Nb:STO	0.35	11	0.39	2.6	0.89
FeSeTe	14	4	0.58	0.86	0.96
$\kappa\text{-ET}$	11	6.1	2.9	1.31	0.96
LSCO08	29	9.1	1.2	2.12	0.88

\*Present address: Department of Quantum Matter Physics, University of Geneva, 1205 Geneva, Switzerland.

†Present address: Department of Physics and Hangzhou Key Laboratory of Quantum Matter, Hangzhou Normal University, Hangzhou 311121, China.

‡Present address: National Institute of Advanced Industrial Science and Technology (AIST), Tsukuba 305-8565, Japan.

§Present address: Max Planck Institute for Solid State Research, Heisenbergstrasse 1, 70569 Stuttgart, Germany.

||Present address: H. H. Wills Physics Laboratory, University of Bristol, Tyndall Avenue, Bristol BS8 1TL, United Kingdom.

¶kamran.behnia@espci.fr

- [1] M. Tinkham, *Introduction to Superconductivity* (Courier Corporation, North Chelmsford, MA, 1996).
- [2] G. Blatter, M. V. Feigel'man, V. B. Geshkenbein, A. I. Larkin, and V. M. Vinokur, *Rev. Mod. Phys.* **66**, 1125 (1994).
- [3] K. Behnia and H. Aubin, *Rep. Prog. Phys.* **79**, 046502 (2016).
- [4] R. P. Huebener, *Magnetic Flux Structures in Superconductors* (Springer-Verlag, Berlin, 1979).
- [5] T. T. M. Palstra, B. Batlogg, L. F. Schneemeyer, and J. V. Waszczak, *Phys. Rev. Lett.* **64**, 3090 (1990).
- [6] H.-C. Ri, R. Gross, F. Gollnik, A. Beck, R. P. Huebener, P. Wagner, and H. Adrian, *Phys. Rev. B* **50**, 3312 (1994).
- [7] Y. Wang, L. Li, and N. P. Ong, *Phys. Rev. B* **73**, 024510 (2006).
- [8] K. Behnia, *J. Phys. Condens. Matter* **21**, 113101 (2009).
- [9] O. Cyr-Choinière, R. Daou, F. Laliberté, C. Collignon, S. Badoux, D. LeBoeuf, J. Chang, B. J. Ramshaw, D. A. Bonn, W. N. Hardy *et al.*, *Phys. Rev. B* **97**, 064502 (2018).
- [10] M. J. Stephen, *Phys. Rev. Lett.* **16**, 801 (1966).
- [11] K. Maki, *Physica (Utrecht)* **55**, 124 (1971).
- [12] A. Sergeev, M. Reizer, and V. Mitin, *Europhys. Lett.* **92**, 27003 (2010).
- [13] Y. Kozuka, M. Kim, C. Bell, B. G. Kim, Y. Hikita, and H. Y. Hwang, *Nature (London)* **462**, 487 (2009).
- [14] M. Kim, C. Bell, Y. Kozuka, M. Kurita, Y. Hikita, and H. Y. Hwang, *Phys. Rev. Lett.* **107**, 106801 (2011).
- [15] M. Kim, Y. Kozuka, C. Bell, Y. Hikita, and H. Y. Hwang, *Phys. Rev. B* **86**, 085121 (2012).
- [16] See Supplemental Material at <http://link.aps.org/supplemental/10.1103/PhysRevLett.126.077001> for a presentation of experimental technique and a more detailed discussion of the available data and concepts regarding the Nernst signal above and below the superconducting critical temperature.
- [17] X. Lin, Z. Zhu, B. Fauqué, and K. Behnia, *Phys. Rev. X* **3**, 021002 (2013).
- [18] X.-Q. Li, Z.-L. Li, J.-J. Zhao, and X.-S. Wu, *Chin. Phys. B* **29**, 087402 (2020).
- [19] A. Pourret, H. Aubin, J. Lesueur, C. A. Marrache-Kikuchi, L. Bergé, L. Dumoulin, and K. Behnia, *Nat. Phys.* **2**, 683 (2006).
- [20] J. Chang, N. Doiron-Leyraud, O. Cyr-Choinière, G. Grissonnanche, F. Laliberté, E. Hassinger, J.-P. Reid, R. Daou, S. Pyon, T. Takayama *et al.*, *Nat. Phys.* **8**, 751 (2012).
- [21] F. F. Tafti, F. Laliberté, M. Dion, J. Gaudet, P. Fournier, and L. Taillefer, *Phys. Rev. B* **90**, 024519 (2014).
- [22] I. Ussishkin, S. L. Sondhi, and D. A. Huse, *Phys. Rev. Lett.* **89**, 287001 (2002).
- [23] M. N. Serbyn, M. A. Skvortsov, A. A. Varlamov, and V. Galitski, *Phys. Rev. Lett.* **102**, 067001 (2009).
- [24] K. Michaeli and A. M. Finkel'stein, *Europhys. Lett.* **86**, 27007 (2009).
- [25] A. Pourret, H. Aubin, J. Lesueur, C. A. Marrache-Kikuchi, L. Bergé, L. Dumoulin, and K. Behnia, *Phys. Rev. B* **76**, 214504 (2007).
- [26] P. Spathis, H. Aubin, A. Pourret, and K. Behnia, *Europhys. Lett.* **83**, 57005 (2008).
- [27] A. Yazdani and A. Kapitulnik, *Phys. Rev. Lett.* **74**, 3037 (1995).
- [28] A. Pourret, L. Malone, A. B. Antunes, C. S. Yadav, P. L. Paulose, B. Fauqué, and K. Behnia, *Phys. Rev. B* **83**, 020504(R) (2011).
- [29] G. Y. Logvenov, M. V. Kartsovnik, H. Ito, and T. Ishiguro, *Synth. Met.* **86**, 2023 (1997).
- [30] C. Capan, K. Behnia, J. Hinderer, A. G. M. Jansen, W. Lang, C. Marcenat, C. Marin, and J. Flouquet, *Phys. Rev. Lett.* **88**, 056601 (2002).
- [31] P. K. Kovtun, D. T. Son, and A. O. Starinets, *Phys. Rev. Lett.* **94**, 111601 (2005).
- [32] K. Trachenko and V. V. Brazhkin, *Sci. Adv.* **6**, eaba3747 (2020).
- [33] C. Caroli, P. D. Gennes, and J. Matricon, *Phys. Lett.* **9**, 307 (1964).
- [34] S. He, J. He, W. Zhang, L. Zhao, D. Liu, X. Liu, D. Mou, Y.-B. Ou, Q.-Y. Wang, Z. Li *et al.*, *Nat. Mater.* **12**, 605 (2013).
- [35] A. P. Drozdov, M. I. Erements, I. A. Troyan, V. Ksenofontov, and S. I. Shylin, *Nature (London)* **525**, 73 (2015).
- [36] Y. Cao, V. Fatemi, S. Fang, K. Watanabe, T. Taniguchi, E. Kaxiras, and P. Jarillo-Herrero, *Nature (London)* **556**, 43 (2018).